Brain, Behavior, and Immunity xxx (xxxx) xxx

Contents lists available at ScienceDirect

Brain Behavior and Immunity

journal homepage: www.elsevier.com/locate/ybrbi

Histamine-4 receptor antagonist ameliorates Parkinson-like pathology in the striatum

Qiuyuan Fang [a,1], Helena Xicoy [b,c,1], Junqing Shen [a], Sabina Luchetti [d,e], Di Dai [f], Pei Zhou [a,g], Xin-Rui Qi [h], Gerard J.M. Martens [c], Inge Huitinga [e,i], Dick F. Swaab [d], Chunqing Liu [a,*], Ling Shan [d,*]

[a] College of Medical Laboratory, Dalian Medical University, Dalian, Liaoning 116044, China
[b] Dept. Cell Biology, Radboud Institute for Molecular Life Sciences, Radboud University Medical Centre, Geert Grooteplein Zuid 26-28, 6525 GA Nijmegen, The Netherlands
[c] Dept. Molecular Animal Physiology, Donders Institute for Brain, Cognition and Behaviour, Donders Centre for Neuroscience, Faculty of Science, Geert Grooteplein Zuid 26-28, 6525 GA Nijmegen, The Netherlands
[d] Dept. Neuropsychiatric Disorders, Netherlands Institute for Neuroscience, An Institute of the Royal Netherlands Academy of Arts and Sciences, Meibergdreef 47 1105BA, Amsterdam, The Netherlands
[e] Dept. Neuroimmunology, Netherlands Institute for Neuroscience, An Institute of the Royal Netherlands Academy of Arts and Sciences, Meibergdreef 47 1105BA, Amsterdam, The Netherlands
[f] Technology Centre of Dalian Customs District P.R.China, Dalian, Liaoning 116001, China
[g] Department of Infectious Diseases, Southwest Hospital, Army Medical University, Chongqing 400038, China
[h] Center for Translational Neurodegeneration and Regenerative Therapy, Shanghai Tenth People's Hospital Affiliated to Tongji University School of Medicine, Shanghai 200072, China
[i] Swammerdam Institute for Life Sciences, University of Amsterdam, Amsterdam, The Netherlands

ARTICLE INFO

Keywords:
Parkinson's disease
Postmortem human brain
Striatum
Histamine-4 receptor antagonist
Microglia
α-synuclein
Neurotransmitters

ABSTRACT

Growing evidence indicates that microglia activation and a neuroinflammatory trigger contribute to dopaminergic cell loss in Parkinson's disease (PD). Furthermore, increased density of histaminergic fibers and enhanced histamine levels have been observed in the substantia nigra of PD-postmortem brains. Histamine-induced microglial activation is mediated by the histamine-4 receptor (H_4R). In the current study, gene set enrichment and pathway analyses of a PD basal ganglia RNA-sequencing dataset revealed that upregulation of H_4R was in the top functional category for PD treatment targets. Interestingly, the H_4R antagonist JNJ7777120 normalized the number of nigrostriatal dopaminergic fibers and striatal dopamine levels in a rotenone-induced PD rat model. These improvements were accompanied by a reduction of α-synuclein-positive inclusions in the striatum. In addition, intracerebroventricular infusion of JNJ7777120 alleviated the morphological changes in Iba-1-positive microglia and resulted in a lower tumor necrosis factor-α release from this brain region, as well as in ameliorated apomorphine-induced rotation behaviour. Finally, JNJ7777120 also restored basal ganglia function by decreasing the levels of γ-aminobutyric acid (GABA) and the 5-hydroxyindoleactic acid to serotonin (5-HIAA/5-HT) concentration ratios in the striatum of the PD model. Our results highlight H_4R inhibition in microglia as a promising and specific therapeutic target to reduce or prevent neuroinflammation, and as such the development of PD pathology.

1. Introduction

Loss of nigrostriatal dopaminergic neurons leads to the hallmark motor symptoms in Parkinson's disease (PD) (Damier et al., 1999; Surmeier et al., 2017). In addition, alpha-synuclein inclusion bodies (Lewy bodies) are evident in multiple brain regions of PD patients (Braak et al., 2004; Shan et al., 2012b). Interestingly, in PD postmortem brains, increased density of histaminergic fibers occurs in the substantia

* Corresponding authors at: Netherlands Institute for Neuroscience, KNAW, Meibergdreef 47 1105 BA, Amsterdam, The Netherlands (L. Shan); College of Medical Laboratory, Dalian Medical University, No. 9 West section, Lvshun South Road, Dalian, Liaoning 116044, China (C. Liu).
E-mail addresses: liuchunqing@dmu.edu.cn (C. Liu), L.shan@nin.knaw.nl (L. Shan).
[1] Authors contributed to the work equally.

https://doi.org/10.1016/j.bbi.2020.11.036
Received 28 July 2020; Received in revised form 22 November 2020; Accepted 23 November 2020
Available online 26 November 2020

nigra (Anichtchik et al., 2000) and enhanced histamine levels have been observed in basal ganglia (Rinne et al., 2002). This augmented histamine stimulates pro-inflammatory microglial activity and accelerates the degeneration of dopamine neurons in the substantia nigra of animal models (Rocha et al., 2016, 2014; Vizuete et al., 2000). Indeed, despite the lack of knowledge of the exact primary cause of the disease, a growing body of evidence suggests the presence of a neuroinflammatory trigger and exacerbation of inflammation of microglia that may accelerate dopaminergic cell loss (Daniele et al., 2015; Deleidi and Gasser, 2013; Doorn et al., 2014b, 2014a, 2012; Gao et al., 2002b, 2002a; Sulzer et al., 2017). We have previously shown that a decrease of endogenous histamine by injection of α-fluoromethylhistidine, an irreversible inhibitor of the key enzyme for neuronal histamine synthesis, histidine decarboxylase (HDC), prevented the loss of dopaminergic neurons in the substantia nigra and strongly reduced the rotation behaviour in this PD rat model (Liu et al., 2007).

Four types of histamine receptors ($H_{1\text{-}4}R$) have been identified in the brain (Panula and Nuutinen, 2013). Crucially, antagonists of H_1R and H_4R reduced the levels of tumor necrosis factor-alpha (TNF-α) and interleukin-6 (IL-6) in primary cultures of human microglia (Dong et al., 2014). Furthermore, the H_4R stands out as the primary mediator of histamine-induced microglial modulation in *in vivo* experiments (Dettori et al., 2018; Frick et al., 2016; Zhou et al., 2019). Intracerebroventricular infusion of histamine increases both the number of ionized calcium binding adaptor molecule 1 (Iba-1) microglia and the density of ramifications in the striatum of wild-type adult mice (Frick et al., 2016). Furthermore, an H_4R antagonist blocks the effect of histamine on microglia, whereas an H_1R agonist has no effect (Frick et al., 2016). In addition, after ischemia, systemic and chronic administration of the specific H_4R antagonist JNJ7777120 (JNJ) reduced ischemic brain damage and improved the sensorimotor deficits accompanied by a reduction in the number of Iba-1 positive microglia cells in rat brain (Dettori et al., 2018). Intracerebroventricular infusion of the same drug prevented dopaminergic neuron degeneration and ameliorated the reduction in dopamine levels in the rotenone-induced PD rat model by inhibited the pro-inflammatory phenotype of microglia (i.e., down-regulated expression of CD86, interleukin-1β (IL-1β), and TNF-α) (Zhou et al., 2019).

Before the efficacy of an H_4R antagonist can be tested in PD patients (Schneider, 2019), in this study we performed a systematic analysis of the histaminergic system in the basal ganglia of PD and the effects of targeting the H_4R in an animal model with PD-like striatal pathology.

2. Materials and methods

2.1. Postmortem human brain material

Brain samples were obtained from the Netherlands Brain Bank (NBB, www.brainbank.nl). Permission for brain autopsy and for the use of the brain material and clinical data for research purposes was obtained by the NBB from the patient or next of kin. The diagnosis and staging of PD patients (Braak et al., 2004), and confirmation of absence of neuropathology were performed by systematic neuropathological examination (van de Nes et al., 1998) by a qualified neuropathologist (Prof. Dr. J.M. Rozemuller, Amsterdam UMC, Amsterdam, the Netherlands). Ten freshly frozen tissue samples of the substantia nigra and nine of the putamen from clinically diagnosed and neuropathologically confirmed PD patients were studied, together with ten and nine well-matched controls (matched for age, sex, postmortem delay, CSF-pH (a parameter for agonal state: (Monoranu et al., 2009))) of the same brain areas of patients without neuropsychiatric disorders or neuropathological changes in the brain. A summary of subject demographic information is presented in Supplementary Table 1.

2.2. RNA sequencing analysis

RNA was extracted using the RNeasy Lipid Tissue Mini Kit and the 260/280 ratio was typically above 1.9. RNA sequencing directional library preparation and sequencing with Poly(A) selection was performed by Hudson Alpha Genomic Services Laboratory (Huntsville, AL). Samples underwent sequencing on the HiSeq v4 (PE, 50 bp, 25 M reads), per standard protocol. 16 samples were run over two lanes (3.125 M reads/sample). Data have been deposited under accession number GSE136666. Reads mapping and quantification were performed with the Salmon pipeline (Patro et al., 2017), after raw data quality control performed with the FASTQC tool. Differential expression analysis was performed with the DESeq2 v1.22.2 Bioconductor's package. This is a method for differential analysis of count data from the RNA sequencing analysis, using shrinkage estimation for dispersions and fold changes to improve stability and interpretability of estimates (Anders and Huber, 2010; Love et al., 2014). Regarding validation of the RNA-sequencing data; we have taken the overlap between our RNA-sequencing data and seven published transcriptomic datasets comparing substantia nigra (whole or laser-microcaptured dopaminergic neurons) from PD patients and controls to be a technical validation (Xicoy et al., 2020). Moreover, the histamine-related findings of the present transcriptome-wide RNA-sequencing analysis are consistent with the results of our previous independent qPCR analyses, which showed a downregulation of H_3R-mRNA and an upregulation of H_4R-mRNA in the basal ganglia of PD patients compared to controls (Shan et al., 2012a).

2.3. KEGG pathway enrichment analysis

We performed functional categorization using the bioinformatics database (http://www.genome.ad.jp/kegg/) of Kyoto Encyclopedia of Genes and Genomes (KEGG) enrichment analysis of biological processes. The cluster profiler R package (organism = "hsa", p value Cutoff = 0.01, p Adjust Method = "BH") was used for the pathway enrichment analysis of differential expression genes (p-value < 0.01 and log2FC < -0.5849 or log2FC > 0.5849).

2.4. Gene set enrichment analysis

As we were focusing on the histamine pathway in PD, we also evaluated histamine-related genes using gene set enrichment tests, as performed in (Wright et al., 2017). HDC is expressed mainly in the posterior hypothalamus (Liu et al., 2010), and has very low expression in both the substantia nigra and the putamen (Shan et al., 2012a), and was therefore not included in this analysis. Briefly, we performed the Bioconductor limma parametric multivariate rotation gene set test (ROAST) (Wu et al., 2010) evaluating five different gene sets, the gene ontology (GO) terms "histamine receptor activity" (GO: 0004969), "histamine secretion" (GO:0001821) and "histamine production involved in inflammatory response" (GO:0002349), and the GeneRIF "histamine" and "histaminergic" from Harmonizome (Rouillard et al., 2016). The analysis was run with 10,000 random rotations to obtain more precise statistical results, and significance values were corrected for multiple testing using the Benjamini–Hochberg false discovery rate method (q-values).

2.5. Animals

All experimental protocols conformed to the guidelines of the institutional Animal Care and Use Committee of Dalian Medical University, China. Every effort was made to minimize the number of animals used and their discomfort. The characteristics of animals and housing conditions of male Sprague-Dawley (SD) rats have been described in detail before (Zhou et al., 2019).

Surgery procedures were described in detail in our previous studies (Liu et al., 2008, 2007; Zhou et al., 2019). The substantia nigra lesions

lead to overt behavioral manifestations with moderate dopamine loss and are thus more appropriate for behavioral studies and drug screening (Sindhu et al., 2005). Briefly, in total 2 μl rotenone (R8875, Sigma-Aldrich, St. Louis, MO, USA) (Rot, 6 μg/μl, dissolved in 50% DMSO + 50% polyethylene glycol (PEG400)) was infused into the right SNpc (Bregma point: lateral (L) = 1.6 mm; antero-posterior (AP) = 4.8 mm; and dorso-ventral (DV) = 8.2 mm) at a speed of 1 μl/min. Sham-operated rats received an identical volume of the 50% DMSO + 50% PEG400 vehicle only. A fixed cannula was implanted in the left lateral ventricle (LV) (L = 1.5 mm; AP = 1.0 mm; DV = 3.8 mm) for intracerebroventricular administration of H_4R antagonist (JNJ, J3770, Sigma-Aldrich St. Louis, MO, USA).

The H_4R antagonist JNJ7777120 was reported to have a functional antagonism with high selectivity over other receptors (Thurmond et al., 2004; Zhou et al., 2019). JNJ administration began immediately after the surgery, and continued for three weeks. The putamen (striatum) of the 18 rats used for the present study for the detection of TNF-α, IL-1β, ARG and IGF-1 by an enzyme-linked immunosorbent assay (ELISA) were samples from the pool of 69 animals used in our previous investigation (Zhou et al., 2019). The rest of the adult male SD rats utilized in the present study weighed between 270 and 320 g and were randomly selected for their use in three groups: a vehicle + saline group (n = 14), a rotenone + saline group (Rot; n = 14) and a rotenone + JNJ (5 μg/day) group (Rot + JNJ; n = 13). Immunohistochemistry for tyrosine hydroxylase (TH), α-synuclein and Iba-1 was performed on 6 other animals per group (n = 6/group). And 23 rats (Vehicle + saline (n = 8); Rot (n = 8); Rot + JNJ (n = 7)) were used for high-performance liquid chromatography with tandem mass spectrometry (HPLC-MS/MS). Finally, a group of rats from the immunohistochemistry group (Vehicle + saline (n = 4); Rot (n = 3); Rot + JNJ (n = 3)) and another group of rats, from the HPLC-MS/MS group (Vehicle + saline (n = 2); Rot (n = 4); Rot + JNJ (n = 2)) were used for the apomorphine-induced rotation behavioural test. The HPLC-MS/MS experiments were repeated and confirmed in a separate aliquots. Included in all experiments, whenever possible, were control groups, randomized procedures and blinded analysis.

2.6. Immunohistochemistry and quantifications

The immunohistochemical procedures employed have been published previously (Zhou et al., 2019). The primary antibodies, dilutions and specificity information are provided in Supplementary Table 2. The quantification and optical-density (OD) analyses have also been described in detail in our previous reports (Shan et al., 2018; Zhou et al., 2019). In short, the light intensity was adjusted for unstained control areas for each section. The collected images were transformed into OD images by a standard transformation curve. The integrated OD was calculated by multiplying the percentage of the positive area by the OD of the immunohistochemistry signal. In addition, the OD values for the Iba-1 signal and the area fraction covered by the Iba-1 signal were calculated as in our recent work (Qi et al., 2019).

An Olympus IX-71 microscope with a three-axis motorized stage, video camera and Image J (National Institutes of Health, Bethesda, MD, USA) was equipped for image analysis. Two or three sections of each rat brain from the same striatum area (one out of six slices distributed from rostral to caudal throughout the striatum (between AP = 0.72–1.68 mm) for staining TH, α-synuclein or Iba-1, respectively) were taken for counting and OD measurements. Under 20× magnification, a total area of 1 mm^2 (50% of total area sampling) bright fields on the lesioned side of each stained section was randomly selected for quantification. The number of Iba-1-positive microglia cells and α-synuclein-positive inclusions were counted. Within that region, all Iba-1-positive cells were randomly selected and manually delineated for measuring the cell-body size of Iba-1-positive cells under 100× magnification. For the TH stain, three bright fields in the lesioned and non-lesioned side of each stained section were selected under 20× and taken for quantification. OD analysis was employed for the quantification. This sampling strategy was optimized by the coefficient of variation ((SD/mean) × 100%), which was lower than 10% (calculated by measuring 1 control 3 times).

To avoid subjective bias, all staining, counting and OD measurements were performed while the researchers were blinded with respect to the nature of the tissue.

2.7. ELISA

The brains were stored at −80 °C and thawed slowly in a cryostat to −18 °C. The striatum was dissected and homogenized in 50 μl of phosphate-buffered saline (PBS, 0.01 M, pH7.4). After centrifugation for 20 min at 3000 rpm/min in 4℃, the supernatant was collected. The protein concentration of supernatant was determined by a Bicinchoninic acid (BCA) protein assay kit (Catalog. no. BL521A, Biosharp, Hefei, China) and adjusted to 1g/L equally with PBS. Four ELISA kits from Lengton bioscience, Shanghai, China for TNF-α (Catalog. no. BPE30635) , IL-1β (Catalog. no. BPE30419), ARG-1 (Catalog. no. BPE30633) and IGF-1 (Catalog. no. BPE30653) were used. Samples/standard and Biotin antigen were first seeded in 96 well plates and incubated for 30 min at 37 °C. The plates were incubated with avidin-(Horseradish Peroxidase) HRP and stopped in 2 M sulphuric acid buffer. The absorbance was measured at the wave length of 450 nm by an ELISA plate reader (BioRad × Mark, Microplate Spectrophotometer, Hercules, CA, USA). Standard curve and sample concentration calculations were performed in the ELISA calc software (Logistic Curve with four parameters, AAT Bioquest, Inc. Sunnyvale, CA USA).

2.8. High performance liquid chromatography tandem mass spectrometry (HPLC-MS/MS)

The rats were perfused with saline and the brain tissues were snap frozen on top of dry ice and stored at −80 °C. Briefly, 1 mg thawed striatum samples were homogenized in 5 μl 0.1% formic acid (Analytic grade, 88%, Kermel Tianjin, China) aqueous solution for 30 s and then samples were centrifuged at 14,000 rpm speed in 4 °C for 10 min. The supernatant was filtered by a 0.22 μm filter (Jinteng Experimental Equipment, Tianjin, China). The filtered supernatant was then diluted 250 times (for γ-aminobutyric acid (GABA) and glutamine (GLN) measurements) or 10 times (for dopamine (DA), acetylcholine (ACh), serotonin (5-HT) and its main metabolite 5-hydroxyindoleactic acid (5-HIAA) measurements) in a 0.1% FA solution that was injected (20 ul) into the HPLC-MS/MS system by an auto sampler. All the standardized chemicals for calibrations were purchased from Sigma-Aldrich, St. Louis, USA, except for the ACh (Yuanye Biological Technology, Shanghai, China).

The detailed HPLC-MS/MS procedure, including the quality controls, has been described in our previous publication (Zhou et al., 2019) and was largely based on previous studies (Jin et al., 2005; Wu et al., 2016). To increase the sensitivity, a number of modifications were made and are given in our MethodsX article.

2.9. Apomorphine-induced rotation behavioural test

Because apomorphine-induced rotations and amphetamine-induced rotations are poorly correlated (Björklund and Dunnett, 2019), and we previously used apomorphine-induced rotations (Liu et al., 2008, 2007; Zhou et al., 2019), for comparative reasons we now used the same system (apomorphine-induced rotations). After three weeks of administration of the H_4R antagonist JNJ, rats were subjected to the apomorphine-induced rotation behavioural test. The animals were habituated to the environment for 10 min. Then apomorphine (National Institutes for Food and Drug Control, Beijing, China; 0.5 mg/kg, subcutaneous injection) was injected to induce ipsilateral rotation behaviour (Liu et al., 2008). Each 360° circle rotation was counted, and the counting continued for 60 min or until the rotation stopped.

2.10. Statistical analysis of animal studies

Data of the groups are expressed as mean ± standard error of the mean (S.E.M.). Statistical analyses were carried out using SPSS Statistics version 19.0 (SPSS Inc, Chicago, IL). For all animal datasets the Kolmogorov-Smirnov test was employed to test for normality (P value ≥ 0.08). The statistical power was tested by G*Power 3.1. Sufficient statistical power was retained (α: 0.05; 1-β ≥ 0.80). These means were analysed by one-way ANOVA followed by a Fisher's least significant difference (LSD) post-hoc correction. The figures were drawn with GraphPad Prism version 7.0 (GraphPad Software, San Diego, CA, USA). P values lower than 0.05 (*), lower than 0.01 (**) and lower than 0.001 (***) were considered statistically significant.

3. Results

3.1. Upregulation of H4R mRNA in the basal ganglia of PD patients

In this study, we analysed the mRNA expression profiles in post-mortem substantia nigra and putamen of PD patients in a transcriptome-wide RNA-sequencing study. Upregulation of H_4R was among the top functional categories in gene set enrichment and pathway analyses. RNA sequencing analysis showed that 354 and 261 gene transcripts were differentially expressed in substantia nigra and putamen samples, respectively, from PD patients versus matched controls (submitted under the accession number GSE136666). Among these gene transcripts, two (H_3R and H_4R) out of the five histamine-related transcripts of interest (i.e., H_1R, H_2R, H_3R, H_4R and histamine N-methyltransferase, HNMT) were significantly differentially expressed in PD and control substantia nigra, but not in putamen (Table 1). Specifically in the substantia nigra of PD patients, H_4R mRNA was upregulated (fold change 1.764; 11.8 ± 5.4 vs 24.0 ± 6.3, P < 0.01**, Table 1) and H_3R mRNA was downregulated (fold change 0.616; 17.2 ± 9.6 vs 17.7 ± 6.5, P < 0.01**, Table 1).

The KEGG enrichment analysis of biological processes identified four functional categories enriched among the most significantly differentially expressed transcripts (P < 0.01 and log2FC < -0.5849 or log2FC > 0.5849) in the substantia nigra of PD (Fig. 1A and Supplementary Table 3). The top functional category was the neuroactive ligand-receptor interaction (KEGG ID: 04080), in which the upregulated H_4R (top 4th gene) and the downregulated H_3R (top 7th) were represented (Fig. 1B). The other significantly enriched pathways were all related to the dopaminergic system, i.e., alcoholism (05034), dopaminergic synapse (04728) and cocaine addiction (05030) (Fig. 1A). Only one functional category, the calcium signalling pathway (04020; Table 2), was enriched among the most significantly differentially expressed transcripts from the putamen of PD (Fig. 1C).

Moreover, a target gene set enrichment ROAST test (a hypothesis-driven analysis) revealed that the GO:0001821 - histamine secretion - is significantly correlated regardless of directionality (mixed results, q value = 0.025*, Table 3) with PD in the substantia nigra. Additionally, GeneRIF: histaminergic and GO:0001821 - histamine secretion - showed a trend towards a correlation regardless of directionality (mixed results, nominal P value = 0.044* and 0.026*, respectively, Table 4) in the putamen of PD.

3.2. H_4R antagonist JNJ ameliorated TH-positive fiber degeneration and prevented dopamine reduction in the striatum of PD rats

We tested whether a chronic intracerebroventricular administration of JNJ improves the main nigrostriatal dopamine projection area of the rotenone-lesioned PD rat model. The changes were monitored by TH immunostaining and by determining dopamine levels in the striatum. One-way ANOVA revealed that treatment with the H_4R-antagonist JNJ yielded significant changes in the ratio of TH-positive fibers of the lesioned side versus the non-lesioned side ($F_{(2, 15)} = 11.789$, P < 0.01**, Fig. 2B and C). Subsequent post-hoc analysis of the treatment effects showed that there was a degeneration of 81.05% of the TH-positive fibers in the striatum of rotenone-lesioned rats compared to the vehicle-treated animals (P < 0.001***, Fig. 2B and C). JNJ ameliorated TH-positive fiber degeneration in rotenone-lesioned PD rats (P < 0.01**, Fig. 2B and C). The TH-positive fibers in the striatum were significantly reduced in the JNJ treatment group compared to the vehicle-treated animals (P < 0.05*, Fig. 2B and C).

One-way ANOVA also showed strong changes in dopamine levels following rotenone treatment in the lesioned side of the striatum ($F_{(2, 20)} = 8.828$, P < 0.01**, Fig. 2D). Subsequent post-hoc analyses for the lesioned side demonstrated that the level of dopamine in the striatum of the rotenone group was significantly lower compared to that of the vehicle + saline control group (P < 0.01**, Fig. 2D). The concentration of dopamine in the striatum was increased significantly in the JNJ + rotenone group compared to the rotenone-lesioned group (P < 0.01**, Fig. 2D).

3.3. JNJ reduced the number of Lewy bodies in the striatum of PD rats

We tested further whether a chronic administration of JNJ to the rotenone-lesioned PD rat model improves the pathology α-synuclein-positive inclusions in the striatum. One-way ANOVA showed strong changes in both the number ($F_{(2, 17)} = 0.801$, P < 0.05*, Fig. 2F) and OD ($F_{(2, 15)} = 7.98$, P < 0.01**, Fig. 2G) of α-synuclein-positive inclusions (Lewy body-like structure) under rotenone treatment in the striatum. Subsequent post-hoc analysis of the treatment effects indicated that there was a substantial increase in the number of α-synuclein-positive

Table 1
Statistical summary for the histaminergic genes of interest in the genome-wide differential expression analysis.

SN Genesymbol	Gene_ID	Ensembl	FoldChange	p-value	q-value
HRH1	NM_001098213	ENSG00000196639	0,854	0,518	0,870
HRH2	NM_022304	ENSG00000113749	0,840	0,340	0,779
HRH3	NM_007232	ENSG00000101180	0,616	0,006**	0,203
HRH4	NM_021624	ENSG00000134489	1,764	0,009**	0,239
HNMT	NM_006895	ENSG00000150540	1,105	0,346	0,779
Put			**FoldChange**	**p-value**	**q-value**
HRH1	NM_001098213	ENSG00000196639	0,742	0,253	0,986
HRH2	NM_022304	ENSG00000113749	1,164	0,493	0,999
HRH3	NM_007232	ENSG00000101180	1,362	0,172	0,942
HRH4	NM_021624	ENSG00000134489	1,261	0,370	0,999
HNMT	NM_006895	ENSG00000150540	0,859	0,269	0,986

Statistical summary of the histaminergic genes of interest that were sufficiently expressed for differential expression analysis between PD and control subjects in the substantia nigra (SN) and the putamen (Put). Log2 fold change is indicated with the controls as the reference group, therefore, each of these genes is more highly expressed in PD than in controls. The p-value indicates the nominal significance for each gene in the differential expression analysis. The q-value indicates the multiple testing corrected significance value for each gene.

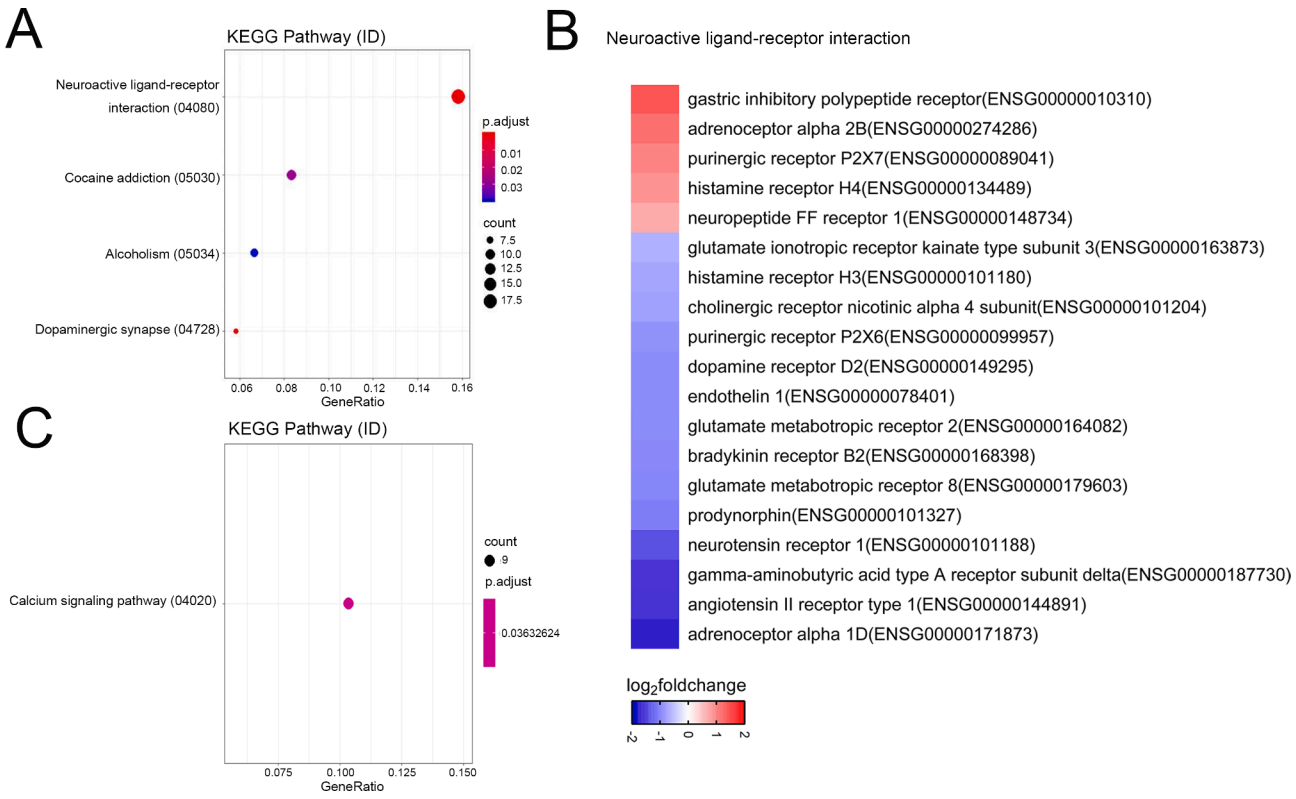

Fig. 1. Biological pathways enriched in both substantia nigra and putamen from PD patients relative to controls. Biological pathways enriched KEGG pathways mapped from 39 top upregulated and 41 top downregulated transcripts in the substantia nigra (A) and in the putamen (C) of the PD. (B) Heatmap showing the expression (log_2 foldchange) of differentially expressed genes of the top enriched gene pathway that show the most significant changes according to their indicated KEGG pathways.

Table 2
Statistical summary for the calcium signaling pathway genes of interest in the genome-wide differential expression analysis.

Gene symbol	Ensembl	FoldChange	p-value	q-value
P2RX7	ENSG00000089041	0,930	0,000278	0,119
P2RX6	ENSG00000099957	−0,861	0,00154	0,224
CASQ1	ENSG00000143318	−1,089	0,00201	0,243
HTR2A	ENSG00000102468	−1,098	0,00449	0,362
MYLK2	ENSG00000101306	−1,133	0,00341	0,322
NOS2	ENSG00000007171	−1,174	0,0000885	0,076
PTGER3	ENSG00000050628	−1,211	0,00412	0,351
PDE1A	ENSG00000115252	−1,447	0,000607	0,151
ADRA1B	ENSG00000170214	−1,495	0,00249	0,281

Statistical summary of the calcium signaling pathway genes of interest that were sufficiently expressed for differential expression analysis between PD and control subjects in the putamen (Put). Log2 fold change is indicated with the controls as the reference group, therefore, each of these genes is more highly expressed in PD than in controls. The p-value indicates the nominal significance for each gene in the differential expression analysis. The q-value indicates the multiple testing corrected significance value for each gene.

inclusions in the striatum of rotenone-lesioned animals compared to the vehicle-treated animals ($P < 0.01$**, Fig. 2E and F). A significant treatment effect of JNJ + rotenone (Fig. 2F) was observed in the number of α-synuclein-positive inclusions in the striatum compared to the rotenone-treated rats ($P < 0.01$**, Fig. 2E and F). Subsequent post-hoc analysis of the treatment effects indicated that there was a significantly higher OD of α-synuclein-positive inclusions in the striatum of rotenone-lesioned rats compared to the vehicle-saline control animals ($P < 0.01$**, Fig. 2E and G). A significant reduction of the OD of α-synuclein-positive inclusions was observed in JNJ + rotenone compared to the rotenone-treated group ($P < 0.01$**, Fig. 2E and G).

3.4. JNJ prevented morphological changes in Iba-1-positive microglia and the protein levels of TNF-α and arginase-1 (ARG) in the striatum of PD rats

To further study the anti-inflammatory role of JNJ, the number and morphology of microglial cells as well as the microglial-mediated inflammation responses were examined. There was no difference in the number ($F_{(2, 15)} = 1.627$, $P > 0.05$, Fig. 3B and C) or densities ($F_{(2, 15)} = 0.446$, $P > 0.05$, Fig. 3B and D) of Iba-1 microglia in the striatum of the three groups (Vehicle + saline, rotenone and rotenone + JNJ) (Fig. 3B and D). One-way ANOVA revealed strong changes in the cell body sizes of Iba-1-positive microglia ($F_{(2, 15)} = 7.267$, $P < 0.01$**, Fig. 3B and E) in the striatum. A clear reduction was present in the sizes of Iba-1-positive microglia in the striatum of the rotenone-lesioned group compared to those of the vehicle-treated animals ($P < 0.05$*, Fig. 3E) and in the striatum of the rotenone-lesioned group compared to the H_4R antagonist JNJ treatment group ($P < 0.01$**, Fig. 3E). In addition, the JNJ treatment normalized the cell sizes of the striatal Iba-1-positive microglia to the control level ($P > 0.05$, Fig. 3E).

One-way ANOVA showed that the protein levels of TNF-α ($F_{(2, 15)} = 3.889$, $P < 0.05$*, Fig. 3F) and ARG ($F_{(2, 14)} = 11.678$, $P < 0.001$***, Fig. 3H) were significantly upregulated, whereas the protein levels of IL-1β ($F_{(2, 15)} = 1.218$, $P > 0.05$, Fig. 3G) and insulin-like growth factor-1 (IGF-1)($F_{(2, 10)} = 0.755$, $P > 0.05$, Fig. 3I) remained unchanged in the striatum of vehicle + saline, rotenone-lesioned PD rats and rotenone + JNJ treated groups. Subsequent post-hoc analyses revealed that the level of TNF-α was significantly upregulated in the striatum of rotenone-lesioned PD rats compared to vehicle + saline-treated rats ($P < 0.05$*, Fig. 3F), while JNJ + rotenone treatment significantly downregulated TNF-α levels ($P < 0.05$*, Fig. 3F). The level of ARG was significantly upregulated in the striatum of rotenone-lesioned PD rats compared to vehicle + saline-treated rats ($P < 0.05$*, Fig. 3H), while JNJ + rotenone

Table 3
Statistical summary for gene set enrichment analysis of the histaminergic genes of interest in substantia nigra.

Substantia nigra								
Gene set	**NGenes**	**PropDown**	**PropUp**	**Direction**	**PValue**	**FDR**	**PValue. Mixed**	**FDR. Mixed**
GO:0001821 - histamine secretion	3	0,333	0,667	Up	0,063	0,313	0,005**	0,025*
GeneRIF: histaminergic	4	0,000	0,250	Up	0,380	0,652	0,463	0,473
GO:0004969 - histamine receptor activity	6	0,167	0,167	Up	0,504	0,652	0,098	0,218
GO:0002349 - histamine production involved in inflammatory response	3	0,333	0,000	Down	0,522	0,652	0,473	0,473
GeneRIF: histamine	75	0,120	0,160	Up	0,845	0,845	0,131	0,218

Summary of results for the gene set enrichment tests of the histaminergic genes. The results are shown with the controls as the reference group. Therefore, the hypothesis of 'Up' refers to the gene set being increased in Parkinson's disease (PD) patients as compared with matched controls. The hypothesis of 'Mixed' refers to the gene set including genes with extreme t-statistics in both directions. Thus, as the results indicate that several of the gene sets show altered expression in PD, the active prop is the proportion of genes in the set contributing meaningfully to significance, defined as those with squared z-values greater than 2. Abbreviation: Direction, direction of change, "Up" or "Down"; FDR, two-sided directional false discovery rate; FDR.Mixed, non-directional false discovery rate; GO, gene ontology; NGenes, number of genes in set; Prop.Down, proportion of genes in set with z < -sqrt(2); Prop.Up, proportion of genes in set with z > sqrt(2); PValue, two-sided directional p-value; PValue.Mixed, non-directional p-value.

Table 4
Statistical summary for gene set enrichment analysis of the histaminergic genes of interest in putamen.

Putamen Gene set	NGenes	PropDown	PropUp	Direction	PValue	FDR	PValue. Mixed	FDR. Mixed
GeneRIF: histaminergic	4,000	0,500	0,000	Down	0,148	0,403	0,044*	0,110
GO:0001821 - histamine secretion	3,000	0,000	0,333	Up	0,161	0,403	0,026*	0,110
GO:0004969 - histamine receptor activity	6,000	0,167	0,000	Down	0,320	0,533	0,379	0,632
GO:0002349 - histamine production involved in inflammatory response	3,000	0,000	0,000	Up	0,845	0,858	0,699	0,699
GeneRIF: histamine	75,000	0,107	0,067	Up	0,858	0,858	0,591	0,699

treatment significantly downregulated ARG levels ($P < 0.01$***, Fig. 3H). Moreover, JNJ + rotenone treatment lowered ARG expression compared to vehicle + saline-treated rats ($P < 0.01$**, Fig. 3H). Furthermore, JNJ + rotenone treatment and rotenone treatment did not significantly change the concentration of IL-1β and IGF-1 compared to vehicle-treated animals (Fig. 3G and I).

3.5. JNJ ameliorated apomorphine-induced rotational behaviour of PD rats

The apomorphine-induced rotation test was employed to explore the JNJ therapeutic effects at the behavioural level. One-way ANOVA revealed strong changes in apomorphine-induced rotational behaviour ($F_{(2,15)} = 4.229$, $P < 0.05$*, Fig. 4B). The rotenone rats displayed a significantly higher apomorphine-induced rotation compared to the vehicle + saline group ($P < 0.05$**, Fig. 4B(b)), while the JNJ + rotenone treatment significantly lowered the apomorphine-induced rotation ($P < 0.05$**, Fig. 4B(b)).

3.6. JNJ affected GABA and 5-HIAA / 5-HT but not GLN and ACh levels in the striatum of PD rats

Not only the dopamine level, but also alterations of GABAergic and cholinergic tones, and a reduced serotonin level have been associated with motor symptoms of PD (Lozovaya et al., 2018; Qamhawi et al., 2015). We also analysed whether JNJ treatment modulates the levels of dopamine and of other neurotransmitters, including GABA, GLN, ACh, 5-HT and 5-HIAA by HPLC-MS/MS. One-way ANOVA showed strong changes of GABA ($F_{(2, 20)} = 11.754$, $P < 0.001$***, Fig. 4C) and 5-HIAA/5-HT ($F_{(2, 20)} = 8.28$, $P < 0.01$**, Fig. 4E) levels under rotenone treatment in the lesioned side of the striatum. There was no difference in the level of GLN ($F_{(2, 20)} = 0.948$, $P > 0.05$, Fig. 4D) or ACh ($F_{(2, 20)} = 2.239$, $P > 0.05$, Fig. 4F) in the striatum among the three groups (Vehicle + saline, rotenone and rotenone + JNJ).

Subsequent post-hoc analyses for the lesioned side demonstrated that the level of GABA and 5-HIAA/5-HT in the striatum were significantly upregulated in the striatum of rotenone-lesioned PD rats compared to vehicle + saline-treated rats ($P < 0.001$***, Fig. 4C; $P < 0.01$**, Fig. 4E), while the JNJ + rotenone treatment significantly lowered the level of GABA ($P < 0.05$* Fig. 4C) as well as the ratio of 5-HIAA/5-HT ($P < 0.01$**, Fig. 4E).

4. Discussion

In this study, we observed the effects of the H_4R antagonist JNJ in a rat model of PD and changes in the basal ganglia histaminergic system of PD patients. Gene set enrichment and pathway analyses of a human basal ganglia RNA-sequencing dataset revealed that H_4R was in the top functional category for PD treatment targets. We subsequently showed, for the first time, that, in the rat striatum, the main dopaminergic nigrostriatal projection area, JNJ inhibited microglial activation and thereby the progression of PD in rotenone-lesioned PD rats. Furthermore, the specific pharmacological targeting of H_4R prevented dopaminergic fiber degeneration, the reduction of the extracellular dopamine level and α-synuclein-positive inclusions in the striatum of the PD rat model. In addition, significant decreases in the size of Iba-1-positive microglia and in the protein level of TNF-α were found in the striatum following JNJ treatment. Moreover, we showed for the first time that blocking H_4R in the striatum of the rotenone-induced PD rodent model suppressed neuroinflammation, prevented dopaminergic neuronal degeneration, and ameliorated the levels of GABA, 5-HT and 5-HIAA without affecting the neurotransmitters GLN and ACh. These H_4R antagonist induced changes were associated with ameliorated apomorphine-induced rotational behaviour.

H_4R-mRNA belongs to the top (4th) genes of "neuroactive ligand-receptor interaction" enriched in the differentially expressed transcripts from the substantia nigra (KEGG ID: 04080). It should be noted that various aspects of the top three from the list - gastric inhibitory polypeptide receptor, adrenoceptor alpha 2B and purinergic receptor P2X7 - have been tested as potential treatments for PD (Athauda et al., 2017; Savola et al., 2003) (ClinicalTrails.gov Id: NCT03918616). However, no information is available on the ability of H_4R antagonists to

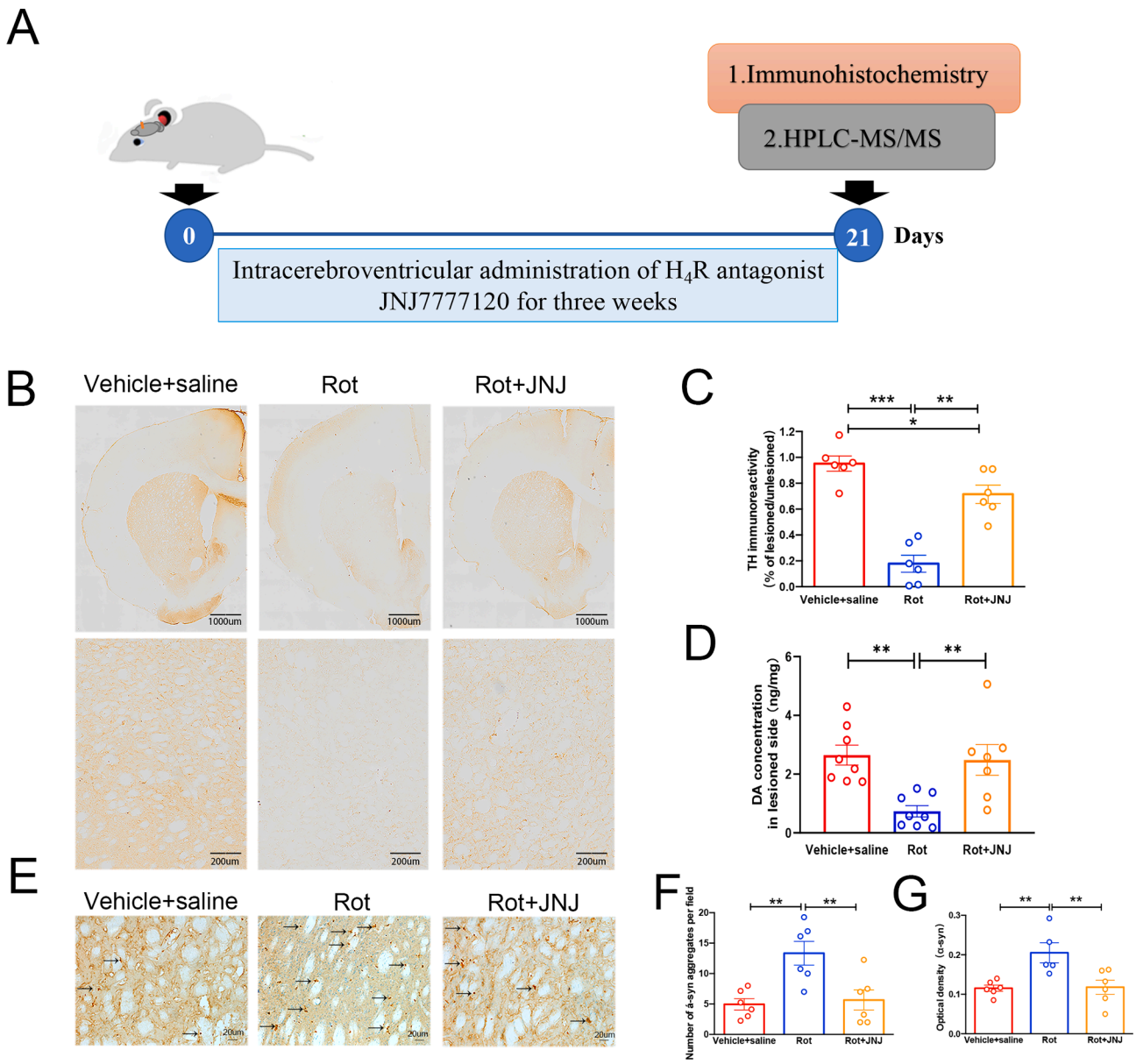

Fig. 2. H_4R antagonist JNJ ameliorated the degeneration of tyrosine hydroxylase (TH) immunoreactive (ir) fibers and prevented the formation of α-synuclein-positive inclusions in the striatum. (A) Schematic diagram of rotenone (Rot) rat model and experimental design. JNJ was infused into the left ventricle for 21 days. Immunohistochemistry and HPLC-MS/MS were performed after 21 days of treatment. (B) Representative images of TH-immunoreactive (ir) fibers of the striatum from 3 groups after three weeks of treatment in the right (lesioned) side of the striatum; (C) Quantification of TH-ir fibers in the striatum of lesioned/unlesioned side; (D) The striatal dopamine (DA) levels. Rotenone (Rot) significantly reduced the TH-ir fibers and decreased the level of DA in striatum, while the fibers and the level of DA significantly augmented under treatment with the H_4R antagonist JNJ. (E) Representative images of α-synuclein-positive inclusions immunostaining in the striatum of 3 groups (Vehicle + saline, Rot; Rot + JNJ). (F) The number of α-synuclein-positive inclusions in the striatum; (G) The α-synuclein-positive inclusion levels were also measured by optical density (OD). There were more α-synuclein-positive inclusions in the striatum in rotenone treated rats, while JNJ significantly reduced the α-synuclein-positive inclusions induced by rotenone. Bar plots show the mean ± S.E.M. The significance of differences from Vehicle + saline or Rot values was calculated using the one-way ANOVA followed by a Fisher's least significant difference (LSD) (*$P < 0.05$, **$P < 0.01$, ***$P < 0.001$).

treat PD. In the present study we therefore tested the possible effect of H_4R antagonists as a novel therapeutic strategy for PD.

In addition, the histamine-related findings of the present transcriptome-wide RNA sequencing is consistent with the results of our previous qPCR analyses which showed a downregulation of H_3R-mRNA in the substantia nigra of PD patients compared to controls (Shan et al., 2012a). H_3R-specific immunohistochemistry showed that this receptor is mainly localized among the large pigmented nigra neurons. The observed H_3R downregulation could thus be largely due to degeneration of the pigmented dopaminergic neurons in the PD substantia nigra (Shan et al., 2012a).

RNA-sequencing of 10 PD cases and 10 controls revealed that H_4R-mRNA is significantly upregulated in the substantia nigra. Our previous qPCR study on 7 PDs and 7 controls has shown that H_4R-mRNA is upregulated but did not reach statistical significance (Shan et al., 2012a). Similarly, our RNA-sequencing data showed upregulation of H_4R-mRNA in the PD putamen, which is in line with our previous qPCR study (Shan et al., 2012a), but the current nominal p-value did not reach significance when corrected for multiple testing.

A large body of evidence supports that histamine regulates microglia activity via the H_4R (Dong et al., 2014; Ferreira et al., 2012; Frick et al., 2016; Zhang et al., 2020; Zhou et al., 2019). H_4R-mRNA have been

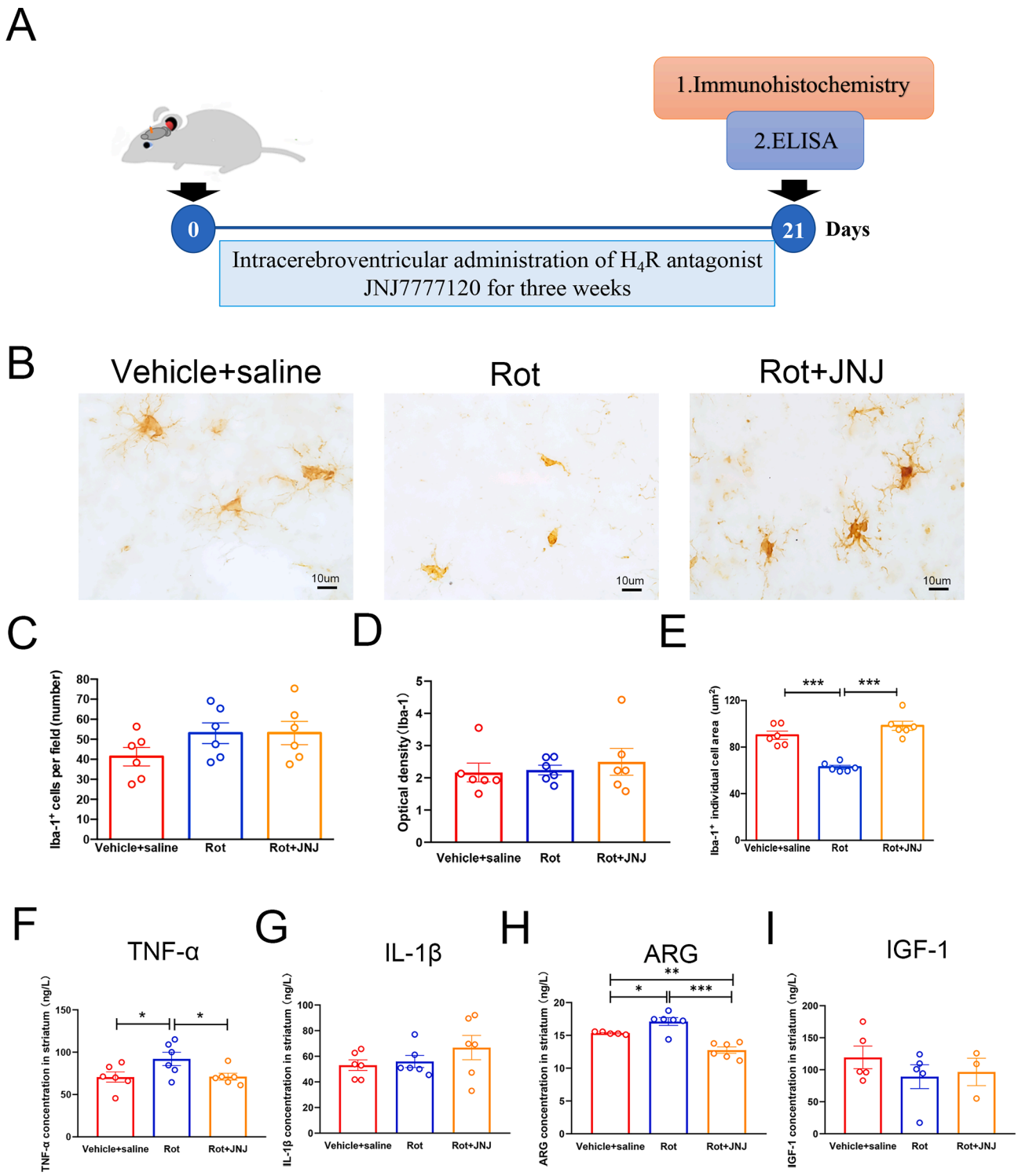

Fig. 3. H_4R antagonist JNJ prevented the morphological changes of Iba-1-positive microglia and suppressed the pro-inflammatory mediator tumour necrosis factor alpha (TNF-a) and Arginine (ARG) levels in the striatum of rotenone-lesioned PD rats. (A) Schematic diagram of rotenone (Rot) rat model and experimental design. JNJ was infused to the left ventricle for 21 days. Immunohistochemistry (B-E) and ELISA (F-I) were performed after 21 days of treatment. (B) Representative immunohistochemistry images of Ionized calcium binding adaptor molecule-1 (Iba-1) in the striatum of 3 groups (Vehicle + saline; rotenone (Rot); Rot + JNJ); (C) Microglia number was stable in the striatum; (D) Optical density of Iba1 immunostaining in striatum was stable; (E) The size of Iba-1-positive microglia decreased significantly in rotenone treated rats, while JNJ significantly increased the size of Iba-1 cells. Shown are the levels of pro-inflammatory mediators (F) Tumour necrosis factor alpha (TNF-a), (G) Interleukine-1 beta (IL-1β), (H) Arginine arginase-1 (ARG) and (I) Insulin like growth factor-1 (IGF-1). Bar plots show the mean ± S.E.M. The significance of differences was calculated using one-way ANOVA followed by a Fisher's least significant difference (LSD) corrections (*P < 0.05, **P < 0.01, ***P < 0.001).

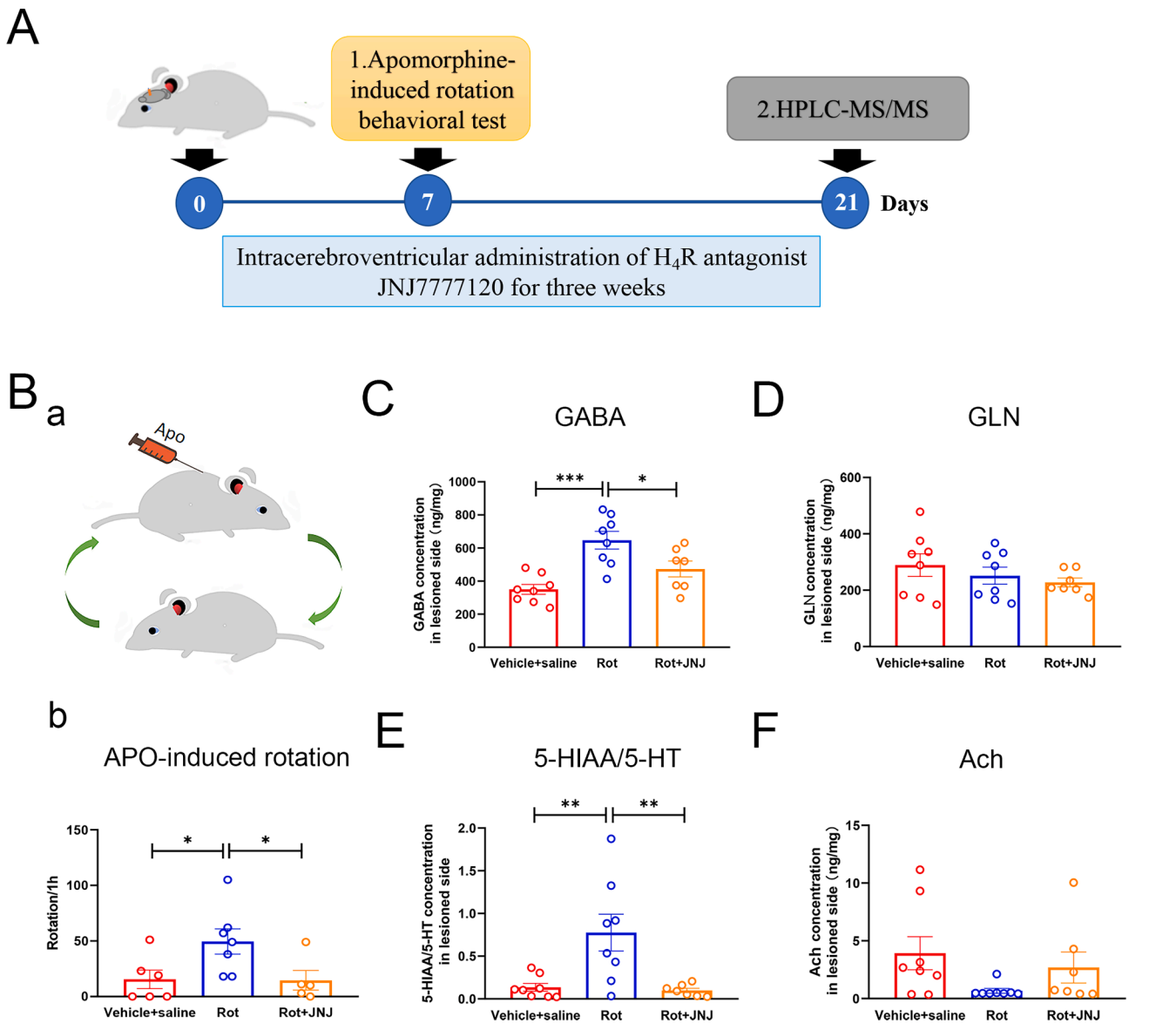

Fig. 4. H_4R antagonist JNJ affected the levels of GABA, GLN, 5-HT/5-HIAA and ACh in the striatum of rotenone-lesioned PD rats. (A) Schematic diagram of rotenone (Rot) rat model and experimental design. JNJ was infused to the left ventricle for 21 days. Apomorphine-induced rotation behavioral test was performed after 7 days (B) and HPLC-MS/MS (C-F) was performed after 21 days of treatment. (B) After one-week of treatment with the H_4R antagonist JNJ7777120 (JNJ), the drug reduced apomorphine (APO)-induced rotation behaviour to control level ((Vehicle + saline (n = 6); rotenone (Rot, n = 7); Rot + JNJ (n = 5)). (C) After three weeks of JNJ-treatment, the level of γ-aminobutyric acid (GABA) (D), glutamine (GLN) (E), serotonin (5-HT) and its main metabolite 5-hydroxyindoleactic acid (5-HIAA) (F), acetylcholine (ACh) were measured by HPLC-MS/MS (Vehicle + saline (n = 8); Rot (n = 8); Rot + JNJ (n = 7)). (C) Rotenone significantly increased the level of GABA in striatum of rats, and JNJ decreased the level of GABA significantly. (D) The effects of rotenone or JNJ treatment on the release of GLN levels in striatum were relatively small. (E) Rotenone significantly increased the ratio of 5-HIAA/5-HT and JNJ decreased the ratio of 5-HIAA/5-HT significantly. (F) Under the rotenone or JNJ treatments, the level of ACh remained relatively stable. The differences between Vehicle + saline and Rot values were calculated using one-way ANOVA followed by a Fisher's least significant difference (LSD) (*P < 0.05, **P < 0.01, ***P < 0.001).

detected in the brain (Connelly et al., 2009; Frick et al., 2016; Strakhova et al., 2009). The commercially available H_4R antibodies lack specificity, preventing immunocytochemical localization (Beermann et al., 2012). However, it should be noted that, as in postmortem human findings, we observed an augmentation of H_4R-mRNA in the rotenone-lesioned PD rat model (Zhou et al., 2019), supporting the use of this PD animal model for the current translational study.

A targeted gene set enrichment analysis using the ROAST test (a hypothesis-driven analysis) revealed that GO:0001821 - histamine secretion - is significantly altered in the substantia nigra of PD. GeneRIF: histaminergic and GO:0001821 - histamine secretion - had a trend towards a differential expression in the putamen of PD. These results are in line with previous postmortem observations of increased density of histaminergic fibers in the substantia nigra (Anichtchik et al., 2000) and enhanced histamine levels in both the substantia nigra and the putamen of PD patients (Rinne et al., 2002). In the current postmortem PD samples we did not observe significant differential expression of gene sets related to inflammation, possibly due to the fact that inflammatory markers are expressed in a time-dependent manner (Simon et al., 2017) and we used samples from the very end stage of PD (the mean disease duration was 16 years). The changes of H_4R in the basal ganglia in the pre-clinical stage of PD patients and a different PD animal model to mimic the pre-clinical stage of PD deserve future study.

We have previously shown that endogenous histamine aggravates degeneration of dopaminergic neurons in the substantia nigra of the 6-hydroxydopamine-lesioned PD rat model (Liu et al., 2007; Shan et al.,

2015). Others have shown that a direct infusion of histamine into the substantia nigra of wild-type rodents mediates the inflammatory response and microglia activation in dopaminergic neuron degeneration (Rocha et al., 2016; Vizuete et al., 2000). H4R antagonist blocks the effects of histamine on microglial cells in the striatum (Frick et al., 2016). In addition, anti-inflammatory effects of the H_4R antagonist JNJ have been reported, including a reduced number of Iba-1-positive microglial cells and decreased levels of pro-inflammatory cytokines such as TNF-α, IL-1β and IL-6 in the rat brain (Dong et al., 2014; Zhang et al., 2020). JNJ-treatment decreased both the mRNA and protein levels of TNF-α and IL-1β and reduced the number of microglia (Zhou et al., 2019). The present study showed that the H_4R antagonist also inhibited the inflammatory process in the striatum of this PD model. JNJ-treatment brought the microglia size back to the control level and normalized the level of TNF-α, without influencing the level of IL-1β and IGF-1. Our present results in the striatum strengthen the notion that H_4R antagonists are a promising novel therapeutic strategy for suppressing the inflammatory responses in the PD brain. Future investigations will include the determination of basal ganglia H_4R changes in the pre-clinical stage of PD postmortem brains and a translational PD animal model study on H_4R that will mimic the pre-clinical stage of PD.

In our experiments, treatment with the H_4R antagonist may have at least partially acted via the inhibition of microglial phagocytosis and suppression of reactive oxygen species production (Rocha et al., 2016). The common pesticide rotenone, an inhibitor of mitochondrial complex I, stimulates microglial phagocytic activity by increasing reactive oxygen species (Emmrich et al., 2013; Gao et al., 2002a; Sherer et al., 2003). In this PD rat model, not only the substantia nigra is severely affected, but also the striatum with its dopaminergic nerve terminals (Betarbet et al., 2000), the area where microglial activation has been observed (Sherer et al., 2003). We did not only find a change in the number of microglia in the substantia nigra (Zhou et al., 2019), but also an alteration in the morphology during striatal microglial aging, something first identified in the brains of aged individuals (Angelova and Brown, 2019; Streit et al., 2004). These changes were characterized by a dystrophic morphology that included process deramification, shortening, gnarling and beading, and the formation of spheroids and cytoplasmic fragmentation (Shaerzadeh et al., 2020). The area differences indicated this dystrophic morphology, which is similar to that of the Rot-treated striatum microglia. In line with our previous study (Zhou et al., 2019), the present work showed that the H_4R antagonist also inhibited the inflammatory process in the striatum of this PD model. JNJ-treatment brought the Iba-1-positive microglia size back to the control level, together with a normalization of the level of inflammation markers such as TNF-α, without influencing the level of IL-1β and IGF-1. Moreover, our RNA-sequencing data showed that the nitric oxide synthase 2 (NOS2/iNOS) gene is significantly downregulated in the putamen of PD. This is an interesting finding, since the H_4R antagonist treatment may act on the reactive oxygen species-mediated regulation of the nitric oxide pathway. Further studies on this topic are thus warranted.

α-synuclein-positive inclusions were observed in the striatum of the rotenone-induced PD rat model, which is consistent with the neuropathology of PD patients (Betarbet et al., 2000; Braak et al., 2003). JNJ treatment ameliorated the α-synuclein-positive inclusions formation in the striatum of the animal model. We have demonstrated previously that this effect was most probably evoked via suppressing activated microglia because JNJ did not prevent PD-like pathology when acting directly on the catecholaminergic neuronal cell line SH-SY5Y (Zhou et al., 2019).

It is known that in the basal ganglia of wild-type rodents, H_3R modulation affects GLN, GABA, 5-HT and Ach levels (Avila-Luna et al., 2019; Ellenbroek and Ghiabi, 2014; Threlfell et al., 2004; Varaschin et al., 2018). However, there was no information regarding the effect of manipulating the histamine receptor H_4R on the levels of neurotransmitters in the basal ganglia. Here we showed for the first time that the H_4R antagonist rescued dopamine levels and recovered levels of GABA and 5-HT and its main metabolite 5-HIAA in basal ganglia of the PD rat model without influencing GLN and Ach levels. These observations reinforce the notion that H_4R antagonists are a promising novel way of intervention in PD.

In summary, this proof of concept study highlights that H_4R-mRNA is upregulated in the substantia nigra of human PD brain samples and that an H_4R antagonist reduced the damaging effects of inflammation in the striatum of a PD rat model. Together with our recent observations (Zhou et al., 2019), the current data pave the way for clinical trials to test the efficacy of H_4R antagonists in PD.

Funding

This work was supported by a grant from the Natural Science Foundation of Liaoning Province, China (2020-MS-254), the National Natural Science Foundation of China, China (31100772) Science and Technology Research General Project of Liaoning Educational Commission, China (L2010102) awarded to Dr. CQ Liu. The Stichting ParkinsonFonds (the Dutch Parkinson's foundation) and Friends of the Netherlands Institute for Neuroscience Foundation funded Dr. L Shan and Prof. D Swaab. Dr. L Shan has received funding through a Marie Skłodowska-Curie grant from the European Union's Horizon 2020 research and innovation programme (Agreement No. 707404).

Declaration of Competing Interest

The authors declare that they have no known competing financial interests or personal relationships that could have appeared to influence the work reported in this paper.

Acknowledgments

The authors are grateful for the valuable discussions with Profs. W. Yang, A-M. Bao and F. Yang from Zhejiang University School of Medicine, Hangzhou, and Dr. D. v. Wamelen from King's College London, and Dr. L Ramanathan from UCLA and W.T.P. Verweij for secretarial assistance.

Contributors

L Shan, CQ Liu, and DF Swaab designed the study. QY Fang, JQ Shen, P Zhou acquired and analysed the animal experiment data. D. Dai acquired and analysed HPLC-MS/MS data. H. Xicoy, G.J.M. Martens and L. Shan acquired and analysed the RNA sequencing data. L. Shan, S. Luchetti, I. Huitinga, G.J.M. Martens and D.F. Swaab wrote the article, which all authors reviewed and approved for publication.

Appendix A. Supplementary data

Supplementary data to this article can be found online at https://doi.org/10.1016/j.bbi.2020.11.036.

References

Angelova, D.M., Brown, D.R., 2019. Microglia and the aging brain: are senescent microglia the key to neurodegeneration? J. Neurochem. 151 (6), 676–688. https://doi.org/10.1111/jnc.14860.

Anichtchik, O.V., Rinne, J.O., Kalimo, H., Panula, P., 2000. An Altered Histaminergic Innervation of the Substantia Nigra in Parkinson's Disease. Exp. Neurol. 163 (1), 20–30. https://doi.org/10.1006/exnr.2000.7362.

Athauda, D., Maclagan, K., Skene, S.S., Bajwa-Joseph, M., Letchford, D., Chowdhury, K., Hibbert, S., Budnik, N., Zampedri, L., Dickson, J., Li, Y., Aviles-Olmos, I., Warner, T. T., Limousin, P., Lees, A.J., Greig, N.H., Tebbs, S., Foltynie, T., 2017. Exenatide once weekly versus placebo in Parkinson's disease: a randomised, double-blind, placebo-controlled trial. The Lancet 390 (10103), 1664–1675. https://doi.org/10.1016/S0140-6736(17)31585-4.

Avila-Luna, A., Ríos, C., Gálvez-Rosas, A., Montes, S., Arias-Montaño, J.-A., Bueno-Nava, A., 2019. Chronic administration of the histamine H3 receptor agonist immepip decreases l-Dopa-induced dyskinesias in 6-hydroxydopamine-lesioned rats. Psychopharmacology 236 (6), 1937–1948. https://doi.org/10.1007/s00213-019-5182-y.

Beermann, S., Seifert, R., Neumann, D., 2012. Commercially available antibodies against human and murine histamine H4-receptor lack specificity. Naunyn-Schmiedeberg's Arch Pharmacol 385 (2), 125–135. https://doi.org/10.1007/s00210-011-0700-4.

Betarbet, R., Sherer, T.B., MacKenzie, G., Garcia-Osuna, M., Panov, A.V., Greenamyre, J. T., 2000. Chronic systemic pesticide exposure reproduces features of Parkinson's disease. Nat Neurosci 3 (12), 1301–1306. https://doi.org/10.1038/81834.

Björklund, A., Dunnett, S.B., 2019. The Amphetamine Induced Rotation Test: A Re-Assessment of Its Use as a Tool to Monitor Motor Impairment and Functional Recovery in Rodent Models of Parkinson's Disease. JPD 9 (1), 17–29. https://doi.org/10.3233/JPD-181525.

Braak, H., Tredici, K.D., Rüb, U., de Vos, R.A.I., Jansen Steur, E.N.H., Braak, E., 2003. Staging of brain pathology related to sporadic Parkinson's disease. Neurobiol. Aging 24 (2), 197–211. https://doi.org/10.1016/S0197-4580(02)00065-9.

Braak, H., Ghebremedhin, E., Rüb, U., Bratzke, H., Del Tredici, K., 2004. Stages in the development of Parkinson's disease-related pathology. Cell Tissue Res 318 (1), 121–134. https://doi.org/10.1007/s00441-004-0956-9.

Connelly, W.M., Shenton, F.C., Lethbridge, N., Leurs, R., Waldvogel, H.J., Faull, R.L., Lees, G., Chazot, P.L., 2009. The histamine H4 receptor is functionally expressed on neurons in the mammalian CNS. Br. J. Pharmacol. 157, 55–63. https://doi.org/BPH227 [pii]10.1111/j.1476-5381.2009.00227.x.

Damier, P., Hirsch, E.C., Agid, Y., Graybiel, A.M., 1999. The substantia nigra of the human brain. I. Nigrosomes and the nigral matrix, a compartmental organization based on calbindin D(28K) immunohistochemistry. Brain 122 (Pt 8, 1421–1436.

Daniele, S.G., Béraud, D., Davenport, C., Cheng, K., Yin, H., Maguire-Zeiss, K.A., 2015. Activation of MyD88-dependent TLR1/2 signaling by misfolded α-synuclein, a protein linked to neurodegenerative disorders. ra45 ra45 Sci. Signal. 8 (376). https://doi.org/10.1126/scisignal.2005965.

Deleidi, M., Gasser, T., 2013. The role of inflammation in sporadic and familial Parkinson's disease. Cell. Mol. Life Sci. 70 (22), 4259–4273. https://doi.org/10.1007/s00018-013-1352-y.

Dettori, I., Gaviano, L., Melani, A., Lucarini, L., Durante, M., Masini, E., Pedata, F., 2018. A selective histamine H4 receptor antagonist, JNJ7777120, is protective in a rat model of transient cerebral ischemia. Front. Pharmacol. 9 https://doi.org/10.3389/fphar.2018.01231.

Dong, H., Zhang, W., Zeng, X., Hu, G., Zhang, H., He, S., Zhang, S., 2014. Histamine Induces Upregulated Expression of Histamine Receptors and Increases Release of Inflammatory Mediators from Microglia. Mol. Neurobiol. 49 (3), 1487–1500. https://doi.org/10.1007/s12035-014-8697-6.

Doorn, K.J., Goudriaan, A., Blits-Huizinga, C., Bol, J.G.J.M., Rozemuller, A.J., Hoogland, P.V.J.M., Lucassen, P.J., Drukarch, B., van de Berg, W.D.J., van Dam, A.-M., 2014a. Increased Amoeboid Microglial Density in the Olfactory Bulb of Parkinson's and Alzheimer's Patients: Microglia in Olfactory Bulb of AD and PD Patients. Brain Pathol. 24 (2), 152–165. https://doi.org/10.1111/bpa.12088.

Doorn, K.J., Lucassen, P.J., Boddeke, H.W., Prins, M., Berendse, H.W., Drukarch, B., van Dam, A.-M., 2012. Emerging roles of microglial activation and non-motor symptoms in Parkinson's disease. Prog. Neurobiol. 98 (2), 222–238. https://doi.org/10.1016/j.pneurobio.2012.06.005.

Doorn, K.J., Moors, T., Drukarch, B., van de Berg, W.DJ., Lucassen, P.J., van Dam, A.-M., 2014b. Microglial phenotypes and toll-like receptor 2 in the substantia nigra and hippocampus of incidental Lewy body disease cases and Parkinson's disease patients. Acta Neuropathol. Commun. 2 (1) https://doi.org/10.1186/s40478-014-0090-1.

Ellenbroek, B.A., Ghiabi, B., 2014. The other side of the histamine H3 receptor. Trends Neurosci. 37 (4), 191–199. https://doi.org/10.1016/j.tins.2014.02.007.

Emmrich, J.V., Hornik, T.C., Neher, J.J., Brown, G.C., 2013. Rotenone induces neuronal death by microglial phagocytosis of neurons. FEBS J. 280 (20), 5030–5038. https://doi.org/10.1111/febs.12401.

Ferreira, R., Santos, T., Gonçalves, J., Baltazar, G., Ferreira, L., Agasse, F., Bernardino, L., 2012. Histamine modulates microglia function. J. Neuroinflammation. 9 (1) https://doi.org/10.1186/1742-2094-9-90.

Frick, L., Rapanelli, M., Abbasi, E., Ohtsu, H., Pittenger, C., 2016. Histamine regulation of microglia: Gene-environment interaction in the regulation of central nervous system inflammation. Brain Behav. Immun. 57, 326–337. https://doi.org/10.1016/j.bbi.2016.07.002.

Gao, H.-M., Hong, J.-S., Zhang, W., Liu, B., 2002a. Distinct Role for Microglia in Rotenone-Induced Degeneration of Dopaminergic Neurons. J. Neurosci. 22 (3), 782–790. https://doi.org/10.1523/JNEUROSCI.22-03-00782.2002.

Gao, H.M., Jiang, J., Wilson, B., Zhang, W., Hong, J.S., Liu, B., 2002b. Microglial activation-mediated delayed and progressive degeneration of rat nigral dopaminergic neurons: relevance to Parkinson's disease. J. Neurochem. 81, 1285–1297.

Jin, C.-L., Yang, L.-X., Wu, X.-H., Li, Q., Ding, M.-P., Fan, Y.-Y., Zhang, W.-P., Luo, J.-H., Chen, Z., 2005. Effects of carnosine on amygdaloid-kindled seizures in Sprague–Dawley rats. Neuroscience 135 (3), 939–947. https://doi.org/10.1016/j.neuroscience:2005.06.066.

Liu, C.-Q., Chen, Z., Liu, F.-X., Hu, D.-N., Luo, J.-H., 2007. Involvement of brain endogenous histamine in the degeneration of dopaminergic neurons in 6-hydroxy-dopamine-lesioned rats. Neuropharmacology 53 (7), 832–841. https://doi.org/10.1016/j.neuropharm.2007.08.014.

Liu, C.-Q., Hu, D.-N., Liu, F.-X., Chen, Z., Luo, J.-H., 2008. Apomorphine-induced turning behavior in 6-hydroxydopamine lesioned rats is increased by histidine and decreased by histidine decarboxylase, histamine H1 and H2 receptor antagonists, and an H3 receptor agonist. Pharmacol. Biochem. Behav. 90 (3), 325–330. https://doi.org/10.1016/j.pbb.2008.03.010.

Lozovaya, N., Eftekhari, S., Cloarec, R., Gouty-Colomer, L.A., Dufour, A., Riffault, B., Billon-Grand, M., Pons-Bennaceur, A., Oumar, N., Burnashev, N., Ben-Ari, Y., Hammond, C., 2018. GABAergic inhibition in dual-transmission cholinergic and GABAergic striatal interneurons is abolished in Parkinson disease. Nat. Commun. 9 (1) https://doi.org/10.1038/s41467-018-03802-y.

Ferrer, I., Al-Saraj, S., Keyvani, K., Schmitt, A., Falkai, P., Schittenhelm, J., Halliday, G., Kril, J., Harper, C., McLean, C., Riederer, P., Roggendorf, W., 2009. pH measurement as quality control on human post mortem brain tissue: a study of the BrainNet Europe consortium. Neuropathol. Appl. Neurobiol. 35, 329–337. https://doi.org/NAN1003 [pii]10.1111/j.1365-2990.2008.01003a.x.

Panula, P., Nuutinen, S., 2013. The histaminergic network in the brain: basic organization and role in disease. Nat. Rev. Neurosci. 14 (7), 472–487. https://doi.org/10.1038/nrn3526.

Patro, R., Duggal, G., Love, M.I., Irizarry, R.A., Kingsford, C., 2017. Salmon provides fast and bias-aware quantification of transcript expression. Nat. Methods 14, 417–419. https://doi.org/10.1038/nmeth.4197.

Qamhawi, Z., Towey, D., Shah, B., Pagano, G., Seibyl, J., Marek, K., Borghammer, P., Brooks, D.J., Pavese, N., 2015. Clinical correlates of raphe serotonergic dysfunction in early Parkinson's disease. Brain 138 (10), 2964–2973. https://doi.org/10.1093/brain/awv215.

Qi, X.R., Kamphuis, W., Shan, L., 2019. Astrocyte Changes in the Prefrontal Cortex From Aged Non-suicidal Depressed Patients. Front. Cell. Neurosci. 13. https://doi.org/10.3389/fncel.2019.00503.

Rinne, J.O., Anichtchik, O. V, Eriksson, K.S., Kaslin, J., Tuomisto, L., Kalimo, H., Roytta, M., Panula, P., 2002. Increased brain histamine levels in Parkinson's disease but not in multiple system atrophy. J. Neurochem. 81, 954–960.

Rocha, S.M., Pires, J., Esteves, M., Graca, B., Bernardino, L., 2014. Histamine: a new immunomodulatory player in the neuron-glia crosstalk. Front. Cell Neurosci. 8, 120. https://doi.org/10.3389/fncel.2014.00120.

Rocha, S.M., Saraiva, T., Cristovao, A.C., Ferreira, R., Santos, T., Esteves, M., Saraiva, C., Je, G., Cortes, L., Valero, J., Alves, G., Klibanov, A., Kim, Y.S., Bernardino, L., 2016. Histamine induces microglia activation and dopaminergic neuronal toxicity via H1 receptor activation. J. Neuroinflammation. 13, 137. https://doi.org/10.1186/s12974-016-0600-010.1186/s12974-016-0600-0 [pii].

Rouillard, A.D., Gundersen, G.W., Fernandez, N.F., Wang, Z., Monteiro, C.D., McDermott, M.G., Ma'ayan, A., 2016. The harmonizome: a collection of processed datasets gathered to serve and mine knowledge about genes and proteins. Database. https://doi.org/10.1093/database/baw100.

Savola, J.M., Hill, M., Engstrom, M., Merivuori, H., Wurster, S., McGuire, S.G., Fox, S.H., Crossman, A.R., Brotchie, J.M., 2003. Fipamezole (JP-1730) is a potent α2 adrenergic receptor antagonist that reduces levodopa-induced dyskinesia in the MPTP-lesioned primate model of Parkinson's disease. Mov. Disord. 18, 872–883. https://doi.org/10.1002/mds.10464.

Schneider, E.H., 2019. Microglial histamine H4R in the pathophysiology of Parkinson's disease—a new actor on the stage? Naunyn-Schmiedeberg's Arch. Pharmacol. 392 (6), 641–645. https://doi.org/10.1007/s00210-019-01635-0.

Shaerzadeh, F., Phan, L., Miller, D., Dacquel, M., Hachmeister, W., Hansen, C., Bechtle, A., Tu, D., Martcheva, M., Foster, T.C., Kumar, A., Streit, W.J., Khoshbouei, H., 2020. Microglia senescence occurs in both substantia nigra and ventral tegmental area. Glia 68, 2228–2245. https://doi.org/10.1002/glia.23834.

Shan, L., Bao, A.-M., Swaab, D.F., 2015. The human histaminergic system in neuropsychiatric disorders. Trends Neurosci. 38 (3), 167–177. https://doi.org/10.1016/j.tins.2014.12.008.

Shan, L., Bossers, K., Luchetti, S., Balesar, R., Lethbridge, N., Chazot, P.L., Bao, A.-M., Swaab, D.F., 2012a. Alterations in the histaminergic system in the substantia nigra and striatum of Parkinson's patients: a postmortem study. Neurobiol. Aging 33 (7), 1488.e1–1488.e13. https://doi.org/10.1016/j.neurobiolaging.2011.10.016.

Shan, L., Guo, H.-Y., van den Heuvel, C.N.A.M., van Heerikhuize, J., Homberg, J.R., 2018. Impaired fear extinction in serotonin transporter knockout rats is associated with increased 5-hydroxymethylcytosine in the amygdala. CNS Neurosci. Ther. 24 (9), 810–819. https://doi.org/10.1111/cns.12822.

Shan, L., Liu, C.-Q., Balesar, R., Hofman, M.A., Bao, A.-M., Swaab, D.F., 2012b. Neuronal histamine production remains unaltered in Parkinson's disease despite the accumulation of Lewy bodies and Lewy neurites in the tuberomamillary nucleus. Neurobiol. Aging 33 (7), 1343–1344. https://doi.org/10.1016/j.neurobiolaging.2011.01.004.

Sherer, T.B., Betarbet, R., Kim, J.-H., Greenamyre, J.T., 2003. Selective microglial activation in the rat rotenone model of Parkinson's disease. Neurosci. Lett. 341 (2), 87–90. https://doi.org/10.1016/S0304-3940(03)00172-1.

Simon, D.W., McGeachy, M.J., Bayır, H., Clark, R.S.B., Loane, D.J., Kochanek, P.M., 2017. The far-reaching scope of neuroinflammation after traumatic brain injury. Nat. Rev. Neurol. 13 (3), 171–191. https://doi.org/10.1038/nrneurol.2017.13.

Sindhu, K.M., Saravanan, K.S., Mohanakumar, K.P., 2005. Behavioral differences in a rotenone-induced hemiparkinsonian rat model developed following intranigral or median forebrain bundle infusion. Brain Res. 1051 (1-2), 25–34. https://doi.org/10.1016/j.brainres.2005.05.051.

Strakhova, M.I., Nikkel, A.L., Manelli, A.M., Hsieh, G.C., Esbenshade, T.A., Brioni, J.D., Bitner, R.S., 2009. Localization of histamine H4 receptors in the central nervous system of human and rat. Brain Res. 1250, 41–48. https://doi.org/10.1016/j.brainres.2008.11.018S0006-8993(08)02729-7 [pii].

Streit, W.J., Sammons, N.W., Kuhns, A.J., Sparks, D.L., 2004. Dystrophic microglia in the aging human brain. Glia 45 (2), 208–212. https://doi.org/10.1002/glia.10319.

Sulzer, D., Alcalay, R.N., Garretti, F., Cote, L., Kanter, E., Agin-Liebes, J., Liong, C., McMurtrey, C., Hildebrand, W.H., Mao, X., Dawson, V.L., Dawson, T.M., Oseroff, C., Pham, J., Sidney, J., Dillon, M.B., Carpenter, C., Weiskopf, D., Phillips, E., Mallal, S., Peters, B., Frazier, A., Lindestam Arlehamn, C.S., Sette, A., 2017. T cells from patients with Parkinson's disease recognize alpha-synuclein peptides. Nature 546, 656–661. https://doi.org/10.1038/nature22815.

Surmeier, D.J., Obeso, J.A., Halliday, G.M., 2017. Selective neuronal vulnerability in Parkinson disease. Nat Rev Neurosci 18 (2), 101–113. https://doi.org/10.1038/nrn.2016.178.

Threlfell, S., Cragg, S.J., Kallo, I., Turi, G.F., Coen, C.W., Greenfield, S.A., 2004. Histamine H3 receptors inhibit serotonin release in substantia nigra pars reticulata. J. Neurosci. 24, 8704–8710. https://doi.org/24/40/8704 [pii]10.1523/JNEUROSCI.2690-04.2004.

Thurmond, R.L., Desai, P.J., Dunford, P.J., Fung-Leung, W.-P., Hofstra, C.L., Jiang, W., Nguyen, S., Riley, J.P., Sun, S., Williams, K.N., Edwards, J.P., Karlsson, L., 2004. A Potent and Selective Histamine H 4 Receptor Antagonist with Anti-Inflammatory Properties. J. Pharmacol. Exp. Ther. 309 (1), 404–413. https://doi.org/10.1124/jpet.103.061754.

van de Nes, J.A., Kamphorst, W., Ravid, R., Swaab, D.F., 1998. Comparison of beta-protein/A4 deposits and Alz-50-stained cytoskeletal changes in the hypothalamus and adjoining areas of Alzheimer's disease patients: amorphic plaques and cytoskeletal changes occur independently. Acta Neuropathol. 96, 129–138. https://doi.org/10.1007/s004010050872.

Varaschin, R.K., Osterstock, G., Ducrot, C., Leino, S., Bourque, M.-J., Prado, M.A.M., Prado, V.F., Salminen, O., Rannanpää (née Nuutinen), S., Trudeau, L.-E., 2018. Histamine H 3 Receptors Decrease Dopamine Release in the Ventral Striatum by Reducing the Activity of Striatal Cholinergic Interneurons. Neuroscience 376, 188–203. https://doi.org/10.1016/j.neuroscience:2018.01.027.

Vizuete, M.L., Merino, M., Venero, J.L., Santiago, M., Cano, J., Machado, A., 2000. Histamine infusion induces a selective dopaminergic neuronal death along with an inflammatory reaction in rat substantia nigra. J. Neurochem. 75, 540–552.

Wu, D., Lim, E., Vaillant, F., Asselin-Labat, M.L., Visvader, J.E., Smyth, G.K., 2010. ROAST: Rotation gene set tests for complex microarray experiments. Bioinformatics 26, 2176–2182. https://doi.org/10.1093/bioinformatics/btq401.

Wu, J.-L., Yu, S.-Y., Wu, S.-H., Bao, A.-M., 2016. A sensitive and practical RP-HPLC-FLD for determination of the low neuroactive amino acid levels in body fluids and its application in depression. Neurosci. Lett. 616, 32–37. https://doi.org/10.1016/j.neulet.2016.01.024.

Xicoy, H., Brouwers, J.F., Wieringa, B., Martens, G.J.M., 2020. Explorative Combined Lipid and Transcriptomic Profiling of Substantia Nigra and Putamen in Parkinson's Disease. Cells 9, 1966. https://doi.org/10.3390/cells9091966.

Zhang, W., Zhang, X., Zhang, Y., Qu, C., Zhou, X., Zhang, S., 2020. Histamine Induces Microglia Activation and the Release of Proinflammatory Mediators in Rat Brain Via H1R or H4R. J Neuroimmune Pharmacol. 15 (2), 280–291. https://doi.org/10.1007/s11481-019-09887-6.

Zhou, P., Homberg, J.R., Fang, Q., Wang, J., Li, W., Meng, X., Shen, J., Luan, Y.i., Liao, P., Swaab, D.F., Shan, L., Liu, C., 2019. Histamine-4 receptor antagonist JNJ7777120 inhibits pro-inflammatory microglia and prevents the progression of Parkinson-like pathology and behaviour in a rat model. Brain Behav. Immun. 76, 61–73. https://doi.org/10.1016/j.bbi.2018.11.006.